International Journal of GEOMATE, March., 2021, Vol.20, Issue 79, pp. 34-41
ISSN: 2186-2982 (P), 2186-2990 (O), Japan, DOI: https://doi.org/10.21660/2021.79.6291
Geotechnique, Construction Materials and Environment

AUXETIC TWO-DIMENSION MATERIAL WITH MODIFIED PEANUT PATTERN

Boonthum Wongchai

Faculty of Engineering at Sriracha, Kasetsart University, Thailand

*Corresponding Author, Received: 09 Jun 2020, Revised: 07 Jan. 2021, Accepted: 28 Jan. 2021

ABSTRACT: Auxetic materials with negative Poisson's ratio are alternatively used in engineering applications. In engineering design, light-weight auxetic material with low stress and negative Poisson's ratio is the main topic. The peanut pattern can be reduced the weight by decreasing the equivalent density. The unit cell of the peanut pattern lattice can be drilled with four circle holes. In this study, the auxetic two-dimension material with modified peanut pattern is used to study the effect of the pattern geometric shape and the equivalent density on the stress and the Poisson's ratio. A four-circle punched pattern has been designed with the original peanut pattern. The equivalent density will be changed by varying their radius lengths. The results show that, the stress and the Poisson's ratio can be reduced by increasing the radius length. In the other words, by decreasing the equivalent density, the stress and the Poison's ratio is decreased. The parabolic relationship between the radius length and the stress is found with R-square value more than 0.95 similar to the relationship between the radius length and the Poissong's ratio.

Keywords: Auxetic material, Modified peanut pattern, Negative Poisson's ratio, Stress analysis

1. INTRODUCTION

In engineering materials, auxetic materials with negative Poisson's ratio have recently received more attention. The dominant properties of auxetic materials differ from conventional materials. For auxetic materials, the Poisson's ratio is negative and its transverse deformation is increased by applying the tensile force in the axial direction, meanwhile the transverse deformation of convention materials is decreased [1]. For engineering advantage, auxetic materials can be applied with various engineering properties, such as, increasing of shear resistance, energy absorption, crashworthiness, indentation resistance, and energy dissipation ability [2-6].

The first auxetic foam with negative Poisson's ratio was constructed in 1987 [7-9]. Auxetic materials have been developed by various manufacturing. Nowadays, 3D printer is powerful device to create the test specimen and the real work piece. Two-dimensional and three-dimensional auxetic materials can be manufactured using 3D printer [10].

The re-entrant shape and the chiral shape as shown in Fig. 1 are the popular shapes for auxetic materials microstructure design [11-15]. Beam members with bending dominated topologies are commonly used to analyze the auxetic microstructures with these shapes [16-17]. High stress concentration at the sharp corners in the re-entrant and the chiral auxetic microstructures is the main problem in the axetic microstructure design. The orthogonal elliptical hole pattern in solid material as shown in Fig. 2 was developed to reduce the stress concentration at the sharp corner [1,18].

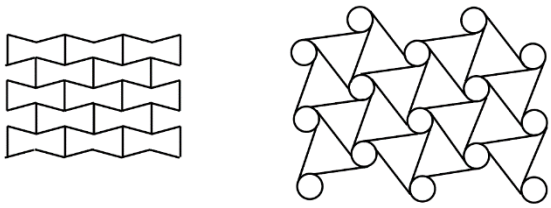

(a) (b)

Fig. 1 Popular shapes of auxetic materials (a) re-entrant shape (b) chiral shape.

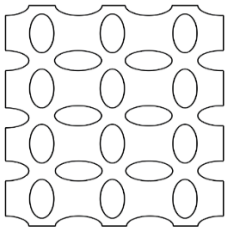

Fig. 2 The orthogonal elliptical hole pattern in solid material.

However, the elliptical pattern also induces high stress too. Hui *et al*., designed the peanut pattern as shown in Fig. 3 with smoothed boundary [1]. By using finite element method, it has been found that the maximum von Mises stress in the peanut pattern is lower than the elliptical hole pattern.

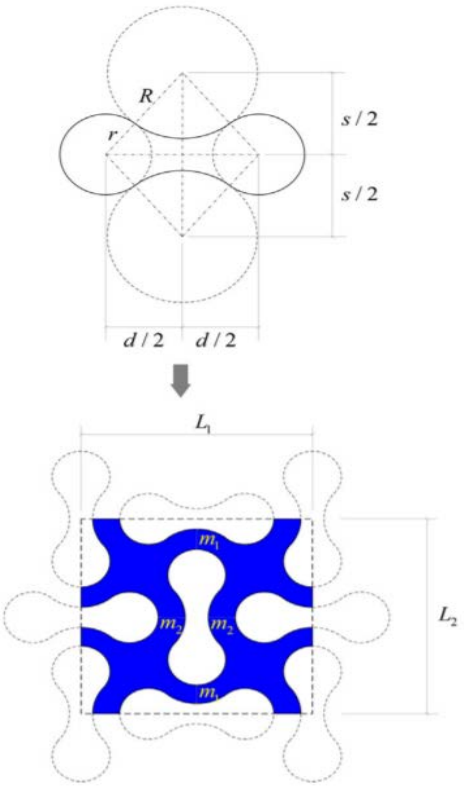

Fig. 3 The peanut pattern [1].

In engineering design, light-weight auxetic material with low stress and negative Poisson's ratio is the main topic. The peanut pattern can reduce the weight by decreasing the equivalent density. The unit cell of the peanut pattern lattice can be drilled with four circle holes. This research purposes to study the effect of the circle hole radius length and the equivalent density of the lattice on the stress and the Poisson's ratio.

2. PATTERN DESIGN

In this study, the original peanut pattern is used from Hui *et al*. research [1]. For reducing the weight, four circle holes are added in the peanut pattern.

2.1 The peanut pattern

For the original peanut pattern as shown in Fig. 3, the centroid distance *s* of the two large circles can be computed by

$$s = 2\sqrt{(r+R)^2 - \frac{d^2}{4}}, \quad (1)$$

where *d* is the centroid distance of the two small circles. It has been assumed that the lengths of the ligaments separating neighboring holes are equal, $m_1 = m_2 = m$, and the side lengths, $L_1 = L_2 = L$, are also equal, The relation is defined as follows,

$$L = d + 2r + s - 2R + 2m \quad (2).$$

The area *A* of each peanut-shaped hole can written as

$$A = 2\pi r^2 + \frac{ds}{2} - 2R^2 \arcsin\left(\frac{d}{2(R+r)}\right) - 2r^2 \arccos\left(\frac{d}{2(R+r)}\right) \quad (3).$$

The equivalent density ρ^* can be evaluated by

$$\frac{\rho^*}{\rho_s} = \frac{L^2 - 4A}{L^2} \quad (4)$$

where ρ_s is the density of the base material [1].

2.2 The modified peanut pattern

The modified peanut pattern is developed from the original peanut pattern with *r* = 2.7 mm, *R* = 7.2 mm, *d* = 10 mm, and *L* = 20 mm. The original peanut lattice is drilled by four-circle holes with radius *a* as shown in Fig. 4.

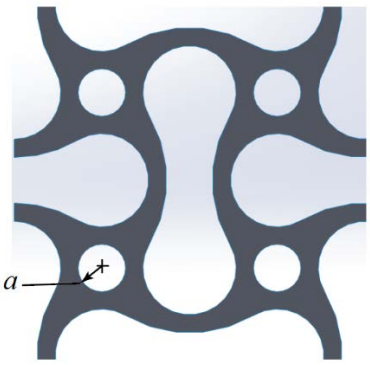

Fig. 4 The modified peanut pattern.

The equivalent density of the modified peanut pattern ρ_1^* can be written by

$$\varphi = \frac{\rho_1^*}{\rho_s} = \frac{L^2 - 4(A + \pi a^2)}{L^2} \quad (5)$$

where φ the equivalent density ratio. In this research, *a* is varied at seven values of *r*/4, *r*/3, *r*/2, 5*r*/8, 11*r*/16, 23*r*/32, and 3*r*/4. It has been noted that,

the maximum value of a is limited at 3r/4 due to its physical structure.

3. STRESS AND POISSON'S RATIO

Finite element method is used to analyze the stress in the auxetic material. The PE high density is used for base materials with Young's modulus of 1.07 GPa, Poisson's ratio of 0.41, tensile strength of 22.10 MPa, and mass density of 952 kg/m^3. The model of the modified peanut pattern with 2×4 array is generated using SOLIDWORKS with thickness of 20 mm. The stress in the auxetic material is computed using SOLIDWORKS Simulation. The boundary conditions are setting with the displacement u_y in y direction at the top edge and fixed at the bottom edge as shown in Fig. 5. The model is meshed using triangular shell element with thickness of 20 mm.

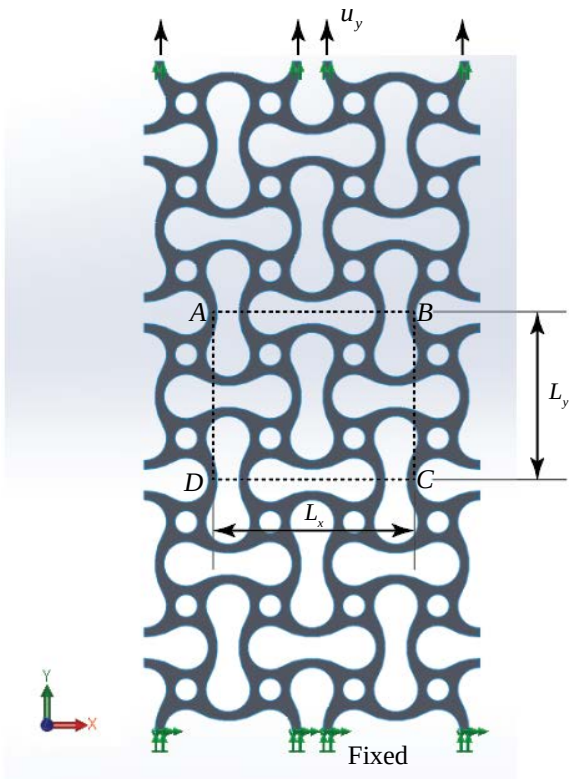

Fig. 5 Boundary conditions.

The maximum von Mises stress $\sigma_{von,\max}$ and the Poisson's ratio ν are computed from the simulation by varying the normal strain ε_y in y direction at 4%, 8%, 12%, 16%, and 24%. For 2×4 unit-cells, the displacement u_y can be determined by

$$\varepsilon_y = \frac{u_y}{4L} \quad (5).$$

The deformation of the rectangular *ABCD* (dash line) is used to determine the Poisson's ratio. By applying the displacement u_y, the original length L_x and L_y are changed to L_x' and L_y' respectively. The Poisson's ratio can be written by

$$\nu = -\frac{(L_y' - L_y)/L_y}{(L_x' - L_x)/L_x} \quad (6).$$

4. RESULT AND DISCUSSION

Fig. 6 shows the von Mises stress in the auxetic material with modified peanut pattern for case of a = $r/4$ and $\varepsilon_y = 8\%$. For all cases, the maximum von Mises stress occurs at the top of the lattice as same as the case of a = $r/4$ and $\varepsilon_y = 8\%$. By varying the radius a and the normal strain ε_y, the maximum von Mises stress for all cases are shown in Table 1.

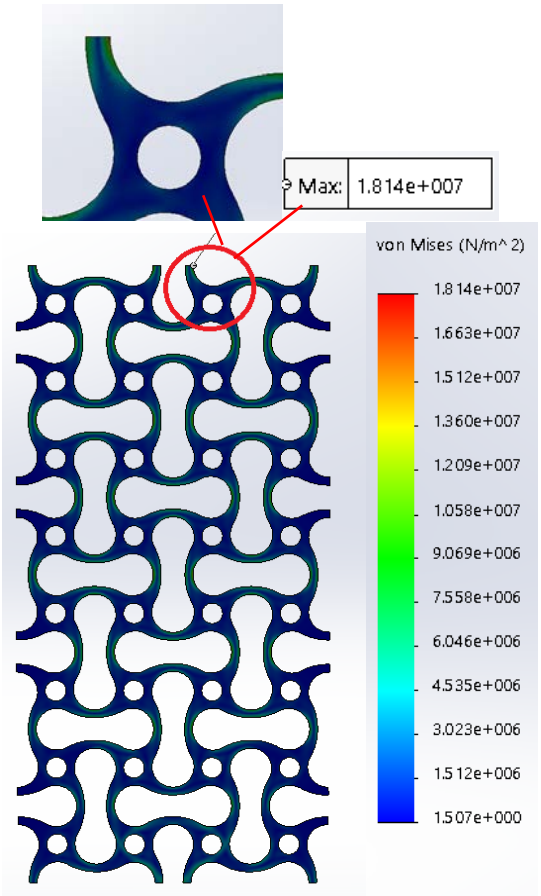

Fig. 6 The von Mises stress in case of a = $r/4$ and $\varepsilon_y = 8\%$.

Table 1. The maximum von Mises stress.

ε_y	$\sigma_{von,\max}$							
	$a = 0$	$a = r/4$	$a = r/3$	$a = r/2$	$a = 5r/8$	$a = 11r/16$	$a = 23r/32$	$a = 3r/4$
4%	8.91	9.146	9.12	8.991	8.687	8.298	7.964	7.43
8%	18.03	18.47	18.42	18.14	17.5	16.69	16	14.91
12%	27.33	27.97	27.88	27.43	26.42	25.15	24.09	22.41
16%	36.81	37.65	37.51	36.87	35.44	33.68	32.22	29.93
20%	46.49	47.49	47.31	46.65	44.56	42.27	40.39	37.47
24%	56.36	57.51	57.27	56.18	53.78	50.92	48.59	45.02

Note: The original peanut-shaped hole pattern has the radius $a = 0$.

Table 2. The percentage change of the maximum von Mises stress compare with the original peanut-shaped hole pattern.

ε_y	$\%\sigma_{von,\max}$ (%)						
	$a = r/4$	$a = r/3$	$a = r/2$	$a = 5r/8$	$a = 11r/16$	$a = 23r/32$	$a = 3r/4$
	$\varphi = 0.39$	$\varphi = 0.38$	$\varphi = 0.35$	$\varphi = 0.31$	$\varphi = 0.30$	$\varphi = 0.29$	$\varphi = 0.27$
4%	2.65	2.36	0.91	-2.50	-6.87	-10.62	-16.61
8%	2.44	2.16	0.61	-2.94	-7.43	-11.26	-17.30
12%	2.34	2.01	0.37	-3.33	-7.98	-11.86	-18.00
16%	2.28	1.90	0.16	-3.72	-8.50	-12.47	-18.69
20%	2.15	1.76	0.34	-4.15	-9.08	-13.12	-19.40
24%	2.04	1.61	-0.32	-4.58	-9.65	-13.79	-20.12
Average	2.32	1.97	0.35	-3.54	-8.25	-12.18	-18.36

Table 3. The Poisson's ratio.

ε_y	ν							
	$a = 0$	$a = r/4$	$a = r/3$	$a = r/2$	$a = 5r/8$	$a = 11r/16$	$a = 23r/32$	$a = 3r/4$
4%	-1.71	-1.70	-1.70	-1.66	-1.60	-1.52	-1.47	-1.38
8%	-1.73	-1.71	-1.72	-1.67	-1.60	-1.52	-1.46	-1.38
12%	-1.73	-1.72	-1.73	-1.67	-1.58	-1.52	-1.46	-1.37
16%	-1.74	-1.73	-1.73	-1.64	-1.60	-1.52	-1.46	-1.31
20%	-1.73	-1.78	-1.72	-1.69	-1.61	-1.52	-1.52	-1.35
24%	-1.74	-1.75	-1.74	-1.69	-1.56	-1.55	-1.45	-1.34
Average	-1.73	-1.78	-1.74	-1.69	-1.57	-1.54	-1.47	-1.33

Table 4. The percentage change of the Poisson's ratio compare with the original peanut-shaped hole pattern.

ε_y	$\%\nu$ (%)						
	$a = r/4$	$a = r/3$	$a = r/2$	$a = 5r/8$	$a = 11r/16$	$a = 23r/32$	$a = 3r/4$
	$\varphi = 0.39$	$\varphi = 0.38$	$\varphi = 0.35$	$\varphi = 0.31$	$\varphi = 0.30$	$\varphi = 0.29$	$\varphi = 0.27$
4%	-0.43	-0.49	-2.87	-6.67	-10.92	-14.19	-19.06
8%	-0.80	-0.42	-3.24	-7.52	-11.75	-15.13	-20.31
12%	-0.39	0.07	-3.36	-8.75	-12.07	-15.68	-20.87
16%	-0.54	-0.08	-3.35	-7.88	-12.20	-16.16	-24.54
20%	0.74	-0.42	-2.36	-7.12	-12.41	-12.11	-21.73
24%	0.53	-0.10	-2.71	-7.39	-10.97	-16.89	-22.73
Average	-0.15	-0.24	-2.98	-7.55	-11.72	-15.03	-21.54

From Table 1, the $\sigma_{von,\max}$ and the ε_y can be plotted with linear trend line as shown in Fig. 7. For cases of $a > r/2$, the results show that the slope of the trend line is less than the original peanut-shaped hole pattern ($a = 0$). In the other words, for $a > r/2$,

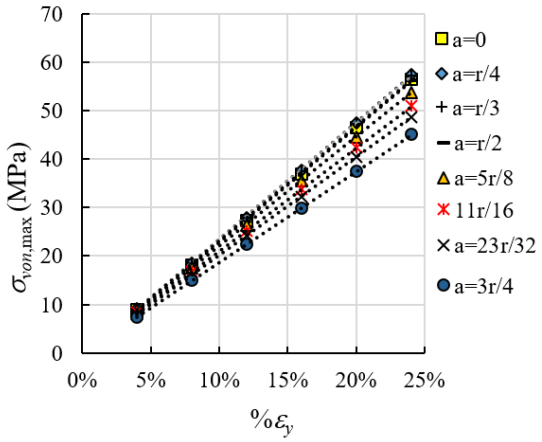

Fig. 7 The maximum von Mises stress-strain curve.

The relationships between the percentage change of maximum von Mises stress $\%\sigma_{von,\max}$ and the normal strain in y direction ε_y are linear trend line with negative slope as shown in Fig. 8. By adding the normal strain in y direction, the percentage change of maximum von Mises stress is reduced. The negative values of the $\%\sigma_{von,\max}$ are occurred when the radius $a > r/2$.

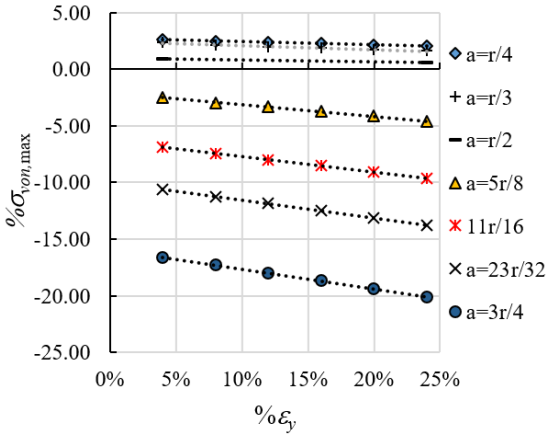

Fig. 8 The percentage change of the maximum von Mises stress versus the normal strain in y direction.

Fig. 9 shows the curve of the $\%\sigma_{von,\max}$ versus the radius a. All curves can be plotted with the parabolic curve. The parabolic curves are very closed to the adjacent curves. Thus, the average of the $\sigma_{von,\max}$ can be reduced by increasing the radius a.

Table 2 shows the percentage change of the maximum von Mises stress compared with the original peanut-shaped hole pattern.
the percentage change of the maximum von Mises stress $\%\sigma_{ave}$ from Table 2 is presented in Fig. 10.

The $\%\sigma_{ave}$ and the radius a can be plotted with the parabolic equation with high R-square as shown in Fig. 10. When $a > 1.46$ mm ($a > 0.54r$), the values of the $\%\sigma_{ave}$ are negative. The $\%\sigma_{ave}$ is rapidly reduced by increasing a small value of the radius a. Thus, by comparing with the original peanut pattern lattice, when $a > 0.54r$, the maximum von Mises stress will be reduced by adding the radius a.

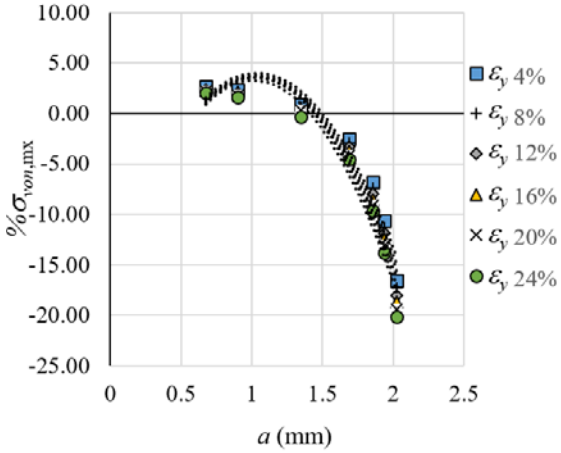

Fig. 9 The percentage change of the maximum von Mises stress versus the radius a.

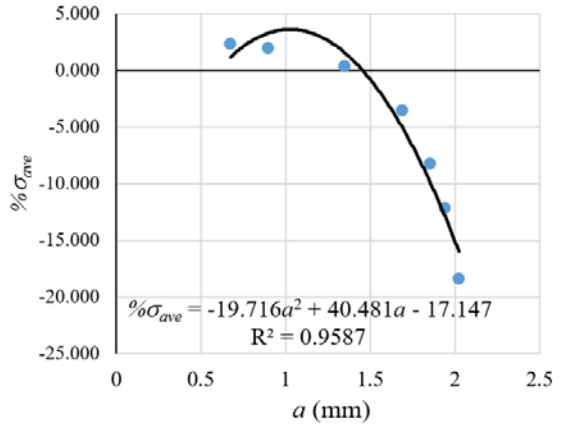

Fig. 10 The average of the percentage change of the maximum von Mises stress versus the radius a.

Fig. 11 shows the parabolic curves of the percentage change of the maximum von Mises stress versus the equivalent density ratio φ. The parabolic curves are very closed to the adjacent

curves. Similar to the curves of the $\%\sigma_{von,\max}$ versus the radius a, the parabolic curve of the $\%\sigma_{ave}$ and the equivalent density ratio φ is presented as shown in Fig. 12. The values of the $\%\sigma_{ave}$ are negative when $\varphi < 0.33$. By reducing of the equivalent density ratio, the average of the percentage change of the maximum von Mises stress is decreased. In the other words, by comparing with the original peanut pattern lattice, the maximum von Mises stress will be reduced when $\varphi < 0.33$. For the constant density of the base material, the maximum von Mises stress can be decreased by reducing the equivalent density of the modified peanut pattern lattice.

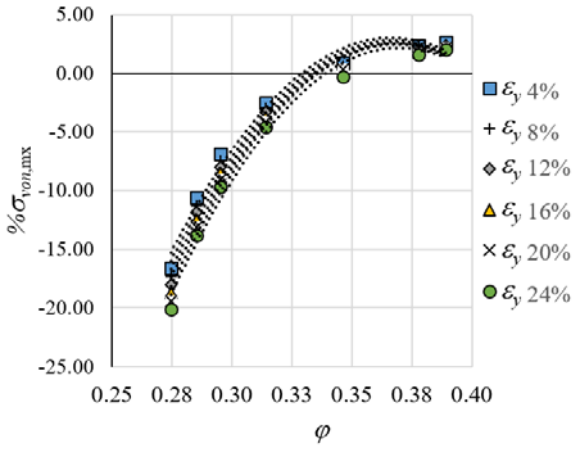

Fig. 11 The percentage change of the maximum von Mises stress versus the equivalent density ratio.

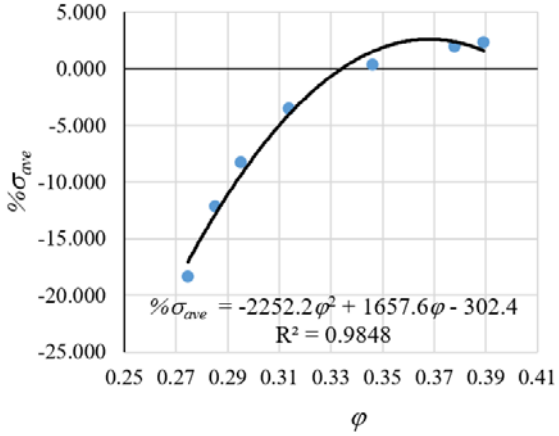

Fig. 12 The average of the percentage change of the maximum von Mises stress versus the equivalent density ratio.

From Table 3, the results show that the negative Poisson's ratio for all cases of the radius a are slightly changed by varying the ε_y. In the other word, the Poisson's ratio is the constant value.

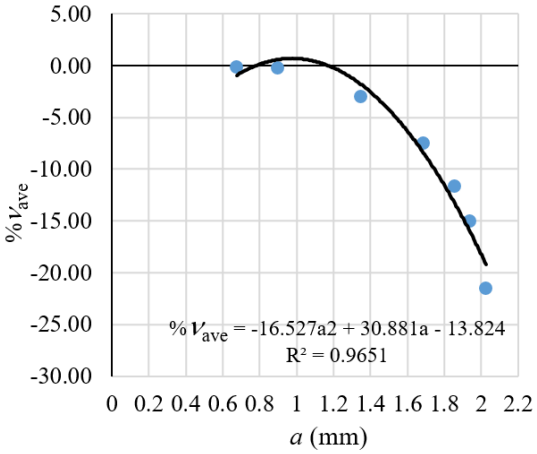

Fig. 13 The average of the percentage change of the Poisson's ratio versus the radius a.

For comparing the Poisson's ratio with the original peanut-shaped hole pattern, the average of the percentage change of the Poisson's ratio $\%\nu_{ave}$ in Table 4 is represented. Fig. 13 shows the parabolic curve of the $\%\nu_{ave}$ versus the radius a with high R-square. When $a > 1.2$ mm ($a > 0.44r$), the $\%\nu_{ave}$ is reduced by adding the radius a.

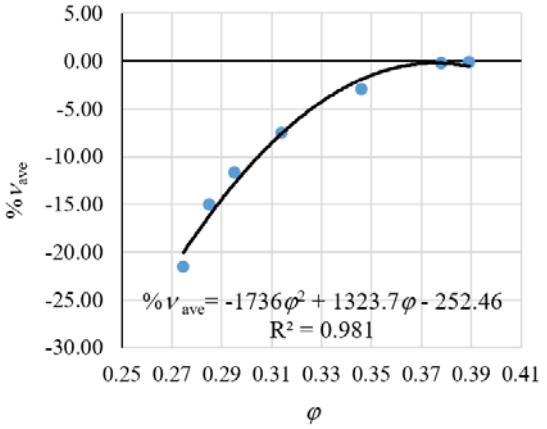

Fig. 14 The average of the percentage change of the Poisson's ratio versus the equivalent density ratio.

From Table 4, the relationship between the $\%\nu_{ave}$ and the equivalent density ratio can be plotted with high R-square parabolic curve as show in Fig. 14. The $\%\nu_{ave}$ is decreased by reducing the equivalent density ratio when $\varphi < 0.37$.

From Figs. 10 and 13, the maximum von Misses stress and the Poisson's ratio can be reduced by adding the radius a meanwhile the maximum von Misses stress and the Poisson's ratio can be reduced by decreasing the equivalent density ratio as shown in Figs. 12 and 14. For the constant density of the base material, the maximum von Misses stress and the Poisson's ratio can be reduced by decreasing the

equivalent density of the modified peanut pattern lattice.

5. CONCLUSION

The relationship between the normal strain in *y* direction and the maximum von Mises stress precisely linear. The experimental results are summarized as follows.

The average of the percentage change of the maximum von Mises stress and the circle hole radius can be plotted with parabolic trend line with high R-square. The average of the percentage change of the maximum von Mises stress is decreased by adding the circle hole radius. Thus, by increasing the circle hole radius, the maximum von Mises stress is reduced.

The curve of the average of the percentage change of the maximum von Mises stress versus the equivalent density ratio of the modified peanut pattern lattice can be plotted with parabolic trend line with high R-square. By reducing of the equivalent density ratio, the average of the percentage change of the maximum von Mises stress is decreased. For constant density of the base material, the maximum von Mises stress is decreased by reducing the equivalent density of the modified peanut pattern lattice.

The average of the percentage change of the Poisson's ratio and the circle hole radius can be plotted with parabolic trend line with high R-square. By increasing the circle hole radius, the average of the percentage change of the Poisson's ratio is reduced. Thus, the Poisson's ratio is decreased by adding the circle hole radius.

The curve of the average of the percentage change of the Poisson's ratio versus the equivalent density ratio of the modified peanut pattern lattice can be plotted with parabolic trend line with high R-square. The average of the percentage change of the Poisson's ratio is increased by reducing of the equivalent density ratio. For constant density of the base material, by decreasing the equivalent density of the modified peanut pattern lattice, the Poisson is increased.

6. REFERENCES

[1] Hui W., Yuxuan Z., Wanqing L., and Qing-Hua Q., A novel two-dimensional mechanical metamaterial with negative Poisson's ratio. Computational Materials Science, Vol. 171, 2020, pp. 1-9.

[2] Yongguang G., Jian Z., Liming C., Bing D., Houchang L., Liliang C., Weiguo L., and Yizhi L., Deformation behaviors and energy absorption of auxetic lattice cylindrical structures under axial crushing load. Aerospace Science and Technology, Vol. 98, 2020, pp. 1-11.

[3] Chong L., Hui-Shen S., Hai Wa., and Zhefeng Y., Large amplitude vibration of sandwich plates with functionally graded auxetic 3D lattice core. International Journal of Mechanical Sciences, Vol. 174, 2020.

[4] Rohit R. M., and Rajib C., Anti-impact behavior of auxetic sandwich structure with braided face sheets and 3D re-entrant cores. Composite Structures, Vol. 236, 2020, pp. 1-16.

[5] Jonathan S., and Zafer K., Crushing investigation of crash boxes filled with honeycomb and re-entrant (auxetic) lattices. Thin-Walled Structures, Vol. 150, 2020, pp. 1-14.

[6] Qingsong W., Zhenyu Y., Zixing L., and Xiang L., Mechanical responses of 3D cross-chiral auxetic materials under uniaxial compression. Materials & Design, Vol. 186, 2020, pp. 1-12.

[7] Yunan P., Seeing auxetic materials from the mechanics point of view: A structural review on the negative Poisson's ratio. Computational Materials Science, Vol. 58, 2013, pp. 140-153.

[8] Mehrdad A., Sanaz S. H., and Akbar R., Auxetic materials materials with negative poisson's ratio. Material Science & Engineering International Journal, Vol. 1, Issue 2, 2017, pp. 62-64.

[9] Carneiro V. H. , Meireles J., and Puga H., Auxetic Materials – A Review. Materials Science-Poland, Vol. 31, Issue 4, 2013, pp. 561-571.

[10] Yuan C., and Qinghao H., 3D-printed short carbon fibre reinforced perforated structures with negative Poisson's ratios: Mechanisms and design. Composite Structures,Vol. 236, 2020, pp. 1-9.

[11] Zeyao C., Xian W., Yi M. X., Zhe W., and Shiwei Z., Re-entrant auxetic lattices with enhanced stiffness: A numerical study. International Journal of Mechanical Sciences, Vol. 178, 2020.

[12] Shengyu D., Li X., Weibin W., and Daining F., A novel design method for 3D positive and negative Poisson's ratio material based on tension-twist coupling effects. Composite Structures, Vol. 236, 2020, pp. 1-16.

[13] Carneiro V. H., Puga H., and Meireles J., Positive, zero and negative Poisson's ratio non-stochastic metallic cellular solids: Dependence between static and dynamic mechanical properties. Composite Structures, Vol. 226, 2020, pp. 1-9.

[14] Xiang-Long P., Celal S., and Swantje B., Phase contrast mediated switch of auxetic mechanism in composites of infilled re-entrant honeycomb microstructures. Extreme Mechanics Letters, Vol. 35, 2020, pp. 1-10.

[15] Zhengyang Z., Hanxing Z., Ru Y., Sanmin W., Tongxiang F., Yacine R., and Di Z., Auxetic interpenetrating composites: A new approach to non-porous materials with a negative or zero Poisson's ratio. Composite Structures, Vol. 243, 2020, pp. 1-8.

[16] Qiang G., Chin A. T., Greg H., and Liangmo W., Geometrically nonlinear mechanical properties of auxetic double-V microstructures with negative Poisson's ratio. European Journal of Mechanics / A Solids, Vol. 80, 2020, pp. 1-11.

[17] Bin L., Kai W., Zhonggang W., Xujing Y., Zhaoliang Q., and Daining F., Experimentally program large magnitude of Poisson's ratio in additively manufactured mechanical metamaterials. International Journal of Mechanical Sciences. Vol. 173, 2020.

[18] Yading X., Hongzhi Z., Erik S., Mladena L., and Branko S., Cementitious cellular composites with auxetic behavior. Cement and Concrete Composites, Vol. 111, 2020, pp. 1-11.

Copyright © Int. J. of GEOMATE. All rights reserved, including the making of copies unless permission is obtained from the copyright proprietors.